

Lattice dynamics of ND_4I in the NaCl phase (I) at 296°K

N. Vagelatos, J. M. Rowe, and J. J. Rush

Institute for Materials Research, National Bureau of Standards, Washington, D. C. 20234

(Received 21 April 1975)

Dispersion curves for translational phonons propagating in the high-symmetry directions of sodium-chloride-phase ND_4I have been determined at room temperature by coherent inelastic neutron scattering from single crystals. Acoustic phonons were well defined throughout the Brillouin zone. Optic phonons were considerably more difficult to measure because of the low signal-to-background ratio. The observed phonon energies were fitted to a "simple" and a "breathing" shell model with general repulsive short-range forces out to second neighbors. The results of the model fitting lead to conclusions similar to those reached in previous alkali halide studies. Model predictions of crystal properties are generally in good agreement with observation. The best fit model was used as an interpolation formula to calculate the density of states, $g(\nu)$. The mean-square displacements are in excellent agreement with those derived from the neutron-diffraction results of Seymour and Pryor. The lattice-dynamics results are compared with similar results obtained recently for the NaCl phases of the alkali cyanides.

I. INTRODUCTION

At atmospheric pressure, the ammonium halides (aside from NH_4F) are known to undergo a number of phase transformations at well-defined transition temperatures.¹ At room temperature NH_4Cl and NH_4Br crystallize with a disordered CsCl structure (phase II), in which the ammonium ions are oriented at random in either of two equivalent orientations in sites with eightfold coordination.² Ammonium iodide, on the other hand, has the NaCl (fcc) structure (phase I) at room temperature in which the NH_4^+ ions are oriented at random in sites with sixfold coordination. NH_4Cl and NH_4Br transform to this phase above 100 °C. At lower temperatures all of these ammonium salts undergo transitions to structures which involve ordering of the NH_4^+ ions. Whereas the two possible orientations in the CsCl phase can be easily visualized, the ammonium ion orientations in phase I are not at all obvious. Extensive investigations of the orientation and dynamical behavior of the ammonium ions in this phase of the ammonium halides by neutron scattering,²⁻¹¹ nuclear magnetic resonance,¹²⁻¹⁵ infrared,^{16,17} Raman,¹⁸ and thermodynamic¹⁹ techniques have led to the viewpoint that (a) the reorientation rate is quite rapid, with an orientational residence time comparable to the period of lattice vibrations^{14,15}; and (b) the motions of the ammonium ions are more complex than either free three-dimensional or single-axis rotation.^{7,12,16} A recent single-crystal neutron-diffraction study of phase-I NH_4I indicates that the average ammonium-ion orientations are such that the proton density has broad maxima in the [100] directions.⁴

The large number of both experimental and theo-

retical studies of the lattice dynamics of the ammonium halides is an indication of the wide interest in these systems. Lattice vibration frequencies have been measured by infrared,^{1,20-22} Raman,^{1,18,23-25} and neutron^{7,11,26-29} techniques; phonon dispersion relations have been calculated on the basis of various lattice-dynamical models³⁰⁻³⁶; and critical-point frequencies have been suggested by maxima in the diffuse inelastic neutron scattering calculated for the disordered phases.³⁷ Only a very small fraction of this work, however, has been concerned with the lattice dynamics of phase I,^{1,21,24,25} where the structure and dynamical disorder make measurements quite difficult.²⁵ In fact, the general result of these studies has been the observation of several broad bands attributed to "one-phonon density-of-states" maxima due to translational phonons.

In the work described here we have measured the crystal dynamics of NaCl-structure ND_4I at room temperature by coherent inelastic neutron scattering from a single crystal. This work provides the first detailed information on the lattice dynamics and crystal force fields in the high-temperature phase of an ammonium halide. These measurements also provide information on the degree to which well-defined phonons exist in this highly disordered phase. In this regard, it should be noted that in a recent neutron study of NaCN and KCN in their analogous disordered NaCl phases,³⁸ it was found that only low-frequency acoustic phonons could be unambiguously measured by coherent inelastic neutron scattering. This lack of clearly observed optic phonons was associated with the orientational disorder of the cyanide ions in the NaCl phase. A comparison of the results for ND_4I and the alkali cyanides should

be useful in assessing the effect of such rotational disorder on the crystal dynamics and character of the phonons in such crystals.

II. EXPERIMENTAL

Single crystals of ND₄I were grown by slow evaporation under controlled conditions from D₂O solutions of deuterated ammonium iodide doped with urea. Deuteration of NH₄I plus urea was accomplished by several H-D exchanges consisting of dissolving the hydrogenous or partly deuterated granular mixture in D₂O, allowing the exchange to reach equilibrium, and evaporating the solvent. Six of seven such exchanges resulted in at least 99% deuteration as indicated by infrared transmission spectra of the evaporated solvent and Raman scattering from the precipitate after the next to the last exchange. Raman scattering from the grown crystals in the NH₄⁺ and ND₄⁺ internal mode frequency range also confirmed the estimate of 99% deuteration. Crystals grown in this manner were parallelepipeds with dimensions up to 2×2×1 cm³. The parallelepiped sides were (100) crystal planes and the mosaic spread was <0.4°.

Coherent inelastic neutron scattering measurements were performed at room temperature (296 °K), using the BT-6 and BT-9 triple axis spectrometers at the NBS reactor. Both of these instruments operate in the fixed incident-energy mode. Incident energies of 14.0, 35.5, 42.5, 60.0, and 75.0 meV were chosen to optimize conditions for the observation of phonons in the different energy ranges. Either beryllium or pyrolytic graphite crystals were used as monochromators, and a graphite filter was used in the 14.0 meV incident energy measurements to eliminate order contamination in the incident beam. Energy analysis of scattered neutrons was performed using either the (002) or (004) planes of pyrolytic graphite crystals. The constant-Q method³⁹ for triple axis spectrometers was primarily used in these measurements. An attempt was also made to measure the far-infrared reflection spectrum for ND₄I, using an interferometer system in the IMR Central Laboratory for Raman and infrared spectroscopy at NBS. This experiment did not provide a satisfactory spectrum, but did yield an independent estimate of the TO and LO frequencies at $q=0$.

III. RESULTS

Dispersion curves were obtained for phonons propagating in the [001], [110], and [111] symmetry directions. The observed phonon energies are listed in Table I, and they are plotted in Fig. 1 together with the results of model calculations

which will be discussed in Sec. IV. Acoustic phonons were well defined, the statistical uncertainties in individual phonon energies generally being (1–3)%. As a result of repeated cross comparison of instrument calibration and target alignment, it is believed that the contribution of systematic errors is negligible. Resolution effects were minimized by careful choice of the scans. Optic phonons were considerably more difficult to measure because of the necessarily worse resolution conditions under which these measurements were performed and the relatively low signal-to-background ratio due to the deuterium incoherent scattering and multiphonon "background." This difficulty is reflected in the larger absolute errors assigned to these phonons. Typical neutron groups are shown in Fig. 2.

Intensity and resolution limitations precluded the observation of the highest-frequency LO phonons, (i.e., near the Brillouin-zone center) and the entire [111] LO branch. A preliminary neutron time-of-flight spectrum measured for ND₄I (discussed below) suggests the absence of well characterized torsional-mode phonons, as does the high degree of rotational disorder revealed by previous studies described above. Thus no attempt was made to investigate rotational or torsional modes by the triple-axis method. It is interesting to note that optic translatory modes as well as acoustic modes near the zone boundary were clearly observed for ND₄I, which were difficult or impossible to observe in the equivalent phase of the alkali cyanide crystals.³⁸ It should also be noted that the ND₄I dispersion curves are qualitatively similar to the dispersion curves of the alkali halides with the NaCl structure,^{40,41} perhaps indicating similar interionic forces. The local minima in the [001] LO and LA branches are characteristic of ionic crystals with highly polarizable components.⁴²

IV. MODEL CALCULATIONS

The ND₄I phonon dispersion data were analyzed in terms of both "simple" and of a "breathing" shell models (SSM and BSM, respectively), by analogy with the previous work on the alkali halides, to obtain the best possible interpolation formula to predict the phonon density of state $g(\nu)$ and related properties. The shell model, originally proposed by Dick and Overhauser,⁴³ has been discussed in detail elsewhere.⁴⁰ The models used in this study follow the formalism of Woods *et al.*⁴⁰ The ND₄⁺ ions are considered to be rigid in that internal modes and their coupling to the lattice modes are neglected. This is a reasonable assumption since the internal mode frequencies are much higher

TABLE I. Measured phonon energies for ND₄I in meV.

[001]						
q/q_{\max}	TA	LA	TO	LO		
0.0			15.90±0.36			
0.1		1.90±0.05				
0.14 ± 0.03		2.75				
0.2	1.06±0.05	3.63±0.05	16.00±0.38	22.00±1.0		
0.27 ± 0.01	1.50			21.00		
0.3	1.56±0.03	5.10±0.05				
0.4	1.93±0.05	6.27±0.04	16.40±0.33	18.30±0.30		
0.5	2.24±0.06	6.60±0.15				
0.6	2.45±0.10	6.70±0.25	16.20±0.30	17.35±0.34		
0.7	2.58±0.08	6.40±0.15				
0.8	2.60±0.08	5.88±0.10	16.50±0.30	17.70±0.40		
0.9	2.70±0.09	5.20±0.12				
1.0	2.65±0.09	4.90±0.12	16.45±0.37	18.00±0.50		
[111]						
q/q_{\max}	TA	LA	TO	LO		
0.0			15.80±0.50			
0.1 ± 0.01	1.50					
0.1		2.50±0.04	16.30±0.70			
0.12 ± 0.02		3.00				
0.15	2.30±0.05					
0.165±0.01		4.00				
0.2	3.00±0.05	4.57±0.05	16.30±0.50	20.30±1.0		
0.26 ± 0.01		5.75				
0.3	4.37±0.05	6.14±0.09				
0.35 ± 0.02		6.75				
0.4	5.54±0.05	7.20±0.20				
0.5	6.12±0.10	7.77±0.20				
[110]						
q/q_{\max}	TA ₂	TA ₁	LA	TO ₂	TO ₁	LO
0.1	0.90±0.05	1.50±0.07	2.23±0.06			
0.15	1.25±0.03	2.32±0.06				
0.2	1.60±0.05	3.13±0.06	4.04±0.08	16.10±0.50	15.25±0.30	
0.3	2.30±0.03	4.68±0.07	5.52±0.06			
0.4	2.92±0.05	5.55±0.07	6.64±0.11	16.40±0.50	15.55±0.30	18.75±0.25
0.5	3.50±0.06	6.05±0.07	7.20±0.11			
0.6	3.96±0.05	5.80±0.15	7.00±0.20	17.00±0.50	15.50±0.30	17.00±0.44
0.7	4.62±0.06	5.14±0.06	6.25±0.10			
0.8	4.70±0.10	4.00±0.05	4.83±0.15	17.6 ± 0.50	15.75±0.40	16.50±0.40
0.9	4.90±0.15	3.08±0.07	3.16±0.10			
1.0	4.90±0.12	2.65±0.09	2.65±0.09			

than the lattice mode frequencies.^{16,18,21} No account was taken of the nonspherical (tetrahedral) shape of the ND₄⁺ ion. Both ions, however, are assumed to be polarizable. Therefore, as in the most general shell models used for the alkali halides, the present SSM has five "electric" parameters, i.e., the I⁻ ion charge Ze , the electronic polarizabilities α_1 and α_2 , and the mechanical deformation charges d_1 and d_2 . The subscripts 1 and 2 refer to the iodine and ammonium ions, respectively. The remaining model parameters describe the repulsive short-range tensor forces between the first- and second-nearest

neighbors. Unlike the models used for the alkali halides, both first- and second-neighbor interactions are assumed to be noncentral. Therefore, the present SSM has eleven short-range parameters. Five of these are the nearest-neighbor force-constant matrix elements or their ratios, $\alpha_R, \gamma_R, \gamma_T, S_R, \gamma_S$, in the notation of Dolling and Waugh.⁴⁴ The remaining six are the second (like) neighbor force-constant matrix elements, $\lambda_1, \lambda_2, \mu_1, \mu_2, \nu_1$, and ν_2 . It is arbitrarily assumed that $\lambda_{1R} = \lambda_{1T} = \lambda_{1S} = \lambda_1$, etc. The BSM which explicitly takes into account the isotropic deformation of the spherical shells, i.e., the variation of the shell

radii, involves exactly the same parameters.^{45,46}

The SSM and BSM were used to fit the observed phonon dispersion curves by a least-squares-fitting code. The results of the best fit 16-parameter models are shown in Fig. 1. Only the neutron data were fitted, unlike previous fits to the alkali halide phonon data which utilized results from neutron, optical, and ultrasonic measurements. Numerous attempts made under further simplifying assumptions to reduce the number of model parameters produced significantly poorer fits to the data. It should be noted that progressively worse agreement was obtained when the following assumptions were implemented: (a) general second-neighbor I⁻ interactions, but no second-neighbor ND₄⁺ interactions (13 parameters); (b) central second-neighbor interactions for both I⁻ and ND₄⁺ ions (14 parameters); and (c) general but equal interactions between I⁻ and ND₄⁺ second-nearest neighbors (13 parameters).

A study of Fig. 1 reveals what has previously been observed in the alkali halide studies. Overall, the SSM fits the phonon dispersion data very well with the exception of the [001] and [110] LO branches. Just as in the alkali halides, the SSM does not predict the dip in the [100] LO branch.⁴⁷ In order to reproduce the shape of this branch more accurately, the assumption of rigid spherical shells (SSM) was abandoned, and the shells of both ions were allowed to "breathe," i.e., to deform isotropically. It can readily be seen in Fig. 1 that the BSM fits the acoustic branches better than the SSM, and, with the possible exception of the TO₁ frequencies, it achieves better agreement with the measured optic modes.

Although some model parameters may assume values which are not physically meaningful be-

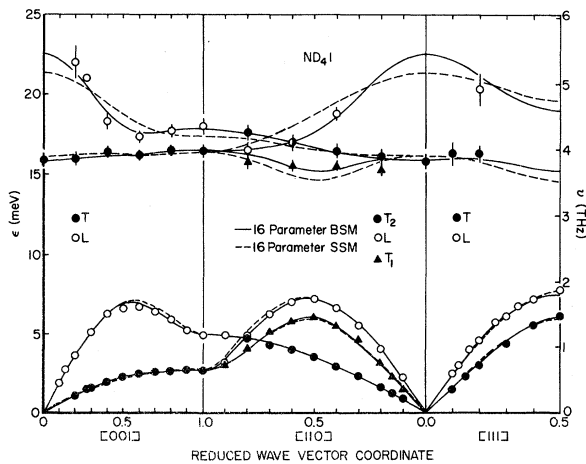


FIG. 1. Phonon dispersion data and 16-parameter SSM and BSM fits for ND₄I. Where no error flags are shown the uncertainties are smaller than the data points.

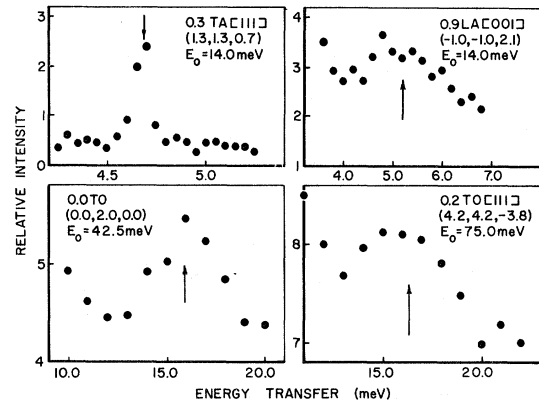


FIG. 2. Typical acoustic and optic neutron groups observed for ND₄I. Corresponding phonon polarization and wave vector are given as well as the neutron wave-vector transfer \vec{Q} and the incident neutron energy.

cause of the large number of parameters and the rather arbitrary assumptions made, it is nevertheless useful to compare the values obtained for ND₄I with the SSM and the BSM, and the published values for KI,⁴¹ since its dispersion curves are qualitatively more similar to the ND₄I curves than those of any other alkali halides. The parameter values are listed in Table II. A comparison of the short-range interaction parameters indicates generally stronger short-range forces for ND₄I, perhaps reflecting differences in the electronic structure of the molecular ND₄⁺ and the K⁺ ions in the iodide crystals. It should be noted that the effective radii of the two ions are quite comparable (1.33 Å for K⁺ and 1.47 Å for ND₄⁺). The SSM

TABLE II. Fitted SSM and BSM parameters for ND₄I and shell-model parameters for KI (Ref. 4).

Parameter	SSM (ND ₄ I)	BSM (ND ₄ I)	SM (KI) ^a
α_R (10^3 dyn/cm)	22.31 ± 1.85	22.29 ± 0.80	18.05 ± 0.67
Z_1 ($ e $)	-1.21 ± 0.08	-0.87 ± 0.08	-0.92 ± 0.04
α_1 (10^{-24} cm ³)	6.62 ± 1.30	5.40 ± 1.02	4.51 ± 0.40
d_1 ($ e $)	0.47 ± 0.08	0.27 ± 0.10	0.13 ± 0.05
α_2 (10^{-24} cm ³)	5.55 ± 1.10	0.05 ± 0.13	2.28 ± 0.14
d_2 ($ e $)	-0.50 ± 0.07	0.05 ± 0.06	-0.11 ± 0.04
S_R	2.55 ± 0.34	3.41 ± 0.70	1
γ_R	-0.09 ± 0.13	-0.08 ± 0.02	-0.07 ± 0.02
γ_T	-0.11 ± 0.02	-0.05 ± 0.05	-0.07 ± 0.02
γ_S	0.03 ± 0.03	0.07 ± 0.05	-0.07 ± 0.02
λ_1 (10^3 dyn/cm)	-1.37 ± 0.25	-0.05 ± 0.54	-0.16 ± 0.17
μ_1 (10^3 dyn/cm)	0.50 ± 0.17	0.61 ± 0.22	0.07 ± 0.07
ν_1 (10^3 dyn/cm)	-0.64 ± 0.25	3.81 ± 1.09	-0.23 ± 0.17
λ_2 (10^3 dyn/cm)	-0.17 ± 0.12	0.21 ± 0.11	-0.11 ± 0.17
μ_2 (10^3 dyn/cm)	-0.24 ± 0.10	-0.40 ± 0.12	-0.01 ± 0.08
ν_2 (10^3 dyn/cm)	0.32 ± 0.21	1.08 ± 0.13	-0.10 ± 0.17
χ^2	3.16	1.62	1.65

^a Reference 41.

and the BSM predict significantly different ionic charges. The BSM value appears to be physically more meaningful, since the ionic charge should be expected to be smaller than the nominal valence charge of -1 . The I^- electronic polarizability α_1 predicted by both models used in the present study agrees reasonably well with the value of 6.43 \AA^3 of Tessman *et al.*⁴⁸ The negative d_2 values are characteristic of shell model fits to the alkali halide phonon dispersion data and are not meaningful within the framework of the shell model formalism, since they imply positive shell charges. Overall, the application of the shell model to the study of the lattice dynamics of ND_4I produces results which are very similar to those obtained for the alkali halides.

The parameter values in Table II were used to derive bulk properties of ND_4I at room temperature. These are listed in Table III together with the corresponding values measured for NH_4I . The elastic constants were calculated using the expressions of Cowley,⁵¹ modified to include the "breathing" terms. They are in reasonable agreement with the observed values in NH_4I ,⁴⁹ and they should be quite comparable since the acoustic-frequency deuterium isotope shift should be $\lesssim 2\%$. The high-frequency dielectric constant ϵ_∞ was determined from the Clausius-Mossotti relation assuming that the electronic polarizability of ND_4I is simply the sum of α_1 and α_2 in Table II. It can be seen in Table III that the SSM predicts a larger value of ϵ_∞ than the BSM. This is due to the fact that the two models predict very different values of the electronic polarizability of the ND_4^+ ions. The compressibility β was calculated from the expression $\beta = 3(C_{11} + 2C_{12})^{-1}$. The predicted values are in good agreement with the observed value in NH_4I .⁵⁰ The assigned uncertainties in the parameter values as well as in the bulk property values derived from them are due to the propagation of the errors in the fitted frequencies.

TABLE III. Bulk properties of ND_4I calculated from SSM and BSM model parameters compared to observed values for NH_4I .

Property	SSM (ND_4I)	BSM (ND_4I)	Observed (NH_4I)
C_{11} (10^{11} dyn/cm ²)	2.82 ± 0.08	2.55 ± 0.03	2.448^a
C_{12} (10^{11} dyn/cm ²)	0.85 ± 0.08	0.74 ± 0.03	0.428^a
C_{44} (10^{11} dyn/cm ²)	0.32 ± 0.02	0.26 ± 0.01	0.240^a
ϵ_0		9.78 ± 11.66	9.8^b
ϵ_∞	4.42 ± 1.27	1.94 ± 0.24	2.90^c
β (10^{-12} cm ² /dyn)	6.62 ± 0.27	7.41 ± 0.13	$\sim 6.6^b$

^a Reference 49.

^b Reference 50.

^c Reference 48.

The BSM was used as an interpolation formula to calculate the translational phonon frequency distribution $g(\nu)$. The computation (based on the extrapolation procedure of Gilat and Raubenheimer⁵⁴) resulted in the phonon density of states shown in Fig. 3. The structure of the calculated $g(\nu)$ displays critical-point and cutoff frequencies, as well as points of high phonon population density, in close agreement with the details of the measured phonon dispersion curves shown in Fig. 1. The polarization vector weighted densities of states for the ND_4^+ and I^- ions were also calculated, and the I^- result is shown as the dashed line in Fig. 3. These partial densities of states were used to calculate the mean-square amplitudes of vibration for both ions at room temperature. The values obtained in this manner are listed in Table IV together with the results of a neutron-diffraction study of room-temperature NH_4I by Seymour and Pryor.⁴ The results of their calculation of the corresponding quantities on the basis of a rigid-ion model fitted only to the compressibility are listed in the same table. The phonon dispersion relations calculated with such a model are expected to bear little resemblance to the present results. These authors suggest that the discrepancies in their neutron-diffraction results and model calculations are due to "displacements of both ions away from their face-centered positions." The agreement between the present calculation on the basis of a more realistic model and the neutron-diffraction result indicates that the large displacements are due only to the thermal motions of the individual ions.

V. DISCUSSION

The present study is one in a series of experiments designed to investigate the effects of high orientational disorder on the lattice dynamics of prototype molecular crystals. The fact that phonon dispersion curves were successfully mea-

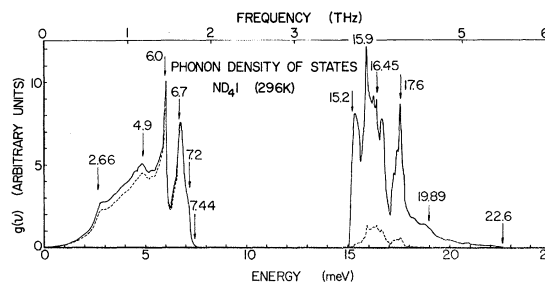


FIG. 3. Translational phonon density of states for ND_4I using the BSM parameter values. Solid line is the total density of states; dash line is the partial density of states for the I^- ion.

sured in ND₄I strongly suggests that the high molecular reorientational rates do not greatly affect translational phonon lifetimes. The source(s) of the difficulties encountered in the alkali cyanide measurements,³⁸ where, for example, no optic phonons were clearly observed, apparently did not exist in the ND₄I experiment, or at least they had only a limited effect on the translational phonons. This suggests that the hindered rotational modes in the alkali cyanides interact more strongly with the translational motions of the neighboring ions, since the rotational modes of the cyanides are expected to have energies (~10 meV) in the range of the translational modes.³⁸ This is in contrast to ND₄I, for which preliminary measurements of the energy distribution of scattered neutrons by the time-of-flight method⁵² show a very broad peak attributed to rotational motions which indicates that such modes have energies in the range ~20–30 meV. It is also possible that the reorientations (as opposed to the hindered rotational modes) of the linear CN⁻ ions affect the lifetimes of the translational vibrations more strongly than the reorientations of the tetrahedral (pseudospherical) ND₄⁺ ions; i.e., the CN⁻ reorientations may induce large ionic displacements which disturb the lattice periodicity. Both of these mechanisms would tend to reduce the phonon lifetimes, or, equivalently, increase the corresponding neutron group widths for molecular crystals having more strongly coupled, lower-frequency rotational motions.

As mentioned above, observation of rotational modes by the triple-axis method was not attempted in this experiment, since well-defined librations apparently do not exist in this system because of the low barrier to rotation (≲5 kJ/mole) and hence the high rate of ND₄⁺ ion reorientation.^{14,15} The lack of clearcut information on the rotational modes, and indeed the uncertainty regarding the nature of the rotational motions and ion orienta-

tions in this system, preclude the analysis of the ND₄I phonon dispersion data in terms of more "complete" models, including rotation-translation coupling, such as those used in the study of the ordered phase of ND₄Cl and NH₄Cl.^{30–36} However, the ability of the "simpler" shell models discussed above to fit the neutron data suggests that in the NaCl phase of the ammonium halides this coupling represents at most a second-order effect.

Finally the results of this measurement should be compared with the limited optical data already published for NH₄I and ND₄I at 296 °K. The present measurement of 15.9 ± 0.3 meV for the TO mode at the Brillouin-zone center is in good agreement with the values of 16.3 ± 0.1 meV,¹ and ~14.8 meV,²¹ derived from infrared transmission measurements. Using their measured value of the TO mode and the dielectric constants listed in Table III, Perry and Lowndes¹ calculated the energy for the LO mode at $q=0$ via the Lyddane-Sachs-Teller (LST) relation. Their value of 29.88 meV is in disagreement with the present neutron data extrapolated to the zone center, and with a preliminary far-infrared reflection measurement which, although not conclusive, indicates that the LO zone-center mode cannot be higher than ≈ 25 meV.⁵³ This disagreement we suspect is most likely due to an incorrect value of ϵ_0 , although it is possible that the simple LST relation is not valid for highly disordered crystals. The interpretation of the one-phonon Raman spectrum for NH₄I (Ref. 24) is reasonably consistent with the neutron data only as far as the acoustic modes are concerned. However, quantitative interpretation of the one-phonon density-of-states spectra was not possible prior to the present study, since the necessary information on the phonon dispersion relations throughout the Brillouin zone was not available.²⁵

The results reported in this paper provide detailed information on the lattice dynamics of the high-temperature phase of an ammonium halide. They show that the high molecular reorientation rate is not the reason for our failure to observe well-defined optic and zone-boundary acoustic phonons in the alkali cyanides, since well-defined phonons were clearly observed in the equivalent phase of ND₄I. The experimental difficulties encountered in the cyanides are instead attributed to the different nature of the reorienting ions (linear versus tetrahedral or pseudospherical) and/or the rotation-translation coupling which should be stronger in the cyanides. This study, however, has not provided information on the nature of the rotational motions of the ammonium ions or the effect of changes of these motions with temperature on the lattice dynamics. We are extending

TABLE IV. Mean-squared displacements calculated from BSM parameters, i.e., using the calculated $g(\nu)$ and polarization vectors, compared to the neutron-diffraction results and rigid-ion model calculation of Seymour and Pryor.

Ion	Present study	$\langle u_x^2 \rangle (\text{\AA}^2)$	
		Neutron diffraction ^a	Rigid ion ^b
Iodide	0.048	0.047 ± 0.001	0.025
Ammonium	0.056	0.054 ± 0.001	0.026

^a Reference 4.

^b Values obtained in Ref. 4 by using a simple rigid-ion model fit *only* to the compressibility of NH₄I.

our phonon measurements in ND_4I and the alkali cyanides to both lower and higher temperatures to probe these effects. It is hoped that more detailed investigations will provide a better understanding of the dynamics of such highly disordered crystals, which include broad groups of

complex inorganic solids and organic plastic crystals.

ACKNOWLEDGMENT

We wish to thank Dr. J. G. Traylor for making available to us the $g(\nu)$ computer code.

- ¹See, e.g., C. H. Perry, and R. P. Lowndes, *J. Chem. Phys.* **51**, 364 (1969).
- ²H. A. Levy and S. W. Peterson, *J. Am. Chem. Soc.* **75**, 1536 (1953).
- ³H. A. Levy and S. W. Peterson, *J. Chem. Phys.* **21**, 366 (1953).
- ⁴R. S. Seymour and A. W. Pryor, *Acta. Crystallogr.* **B 26**, 1487 (1970).
- ⁵G. Venkataraman, K. Usha Deniz, P. K. Iyengar, P. R. Vijayaraghavan, and A. P. Roy, in *Proceedings of the Third International Symposium on Inelastic Scattering of Neutrons*, Bombay (IAEA, Vienna, 1965), Vol. II, p. 347.
- ⁶G. Kosaly and G. Solt, *Physica (Utr.)* **32**, 1571 (1966).
- ⁷G. Venkataraman, K. Usha Deniz, P. K. Iyengar, A. P. Roy, and R. R. Vijayaraghavan, *J. Phys. Chem. Solids* **27**, 1102 (1966).
- ⁸J. J. Rush, T. I. Taylor, and W. W. Havens, Jr., *Phys. Rev. Lett.* **5**, 507 (1960).
- ⁹J. J. Rush, T. I. Taylor, and W. W. Havens, Jr., *J. Chem. Phys.* **37**, 234 (1962).
- ¹⁰V. Brajovic, H. Boutin, G. J. Safford, and H. Palevsky, *J. Phys. Chem. Solids* **24**, 617 (1963).
- ¹¹K. Mikke and A. Kroh, *Inelastic Scattering of Neutrons in Solids and Liquids* (IAEA, Vienna, 1963), Vol. II, p. 237.
- ¹²A. H. Cooke and L. E. Drain, *Proc. Phys. Soc. Lond.* **A 65**, 894 (1952).
- ¹³H. S. Gutowsky, G. E. Pake, and R. Bersohn, *J. Chem. Phys.* **22**, 643 (1954).
- ¹⁴L. Niemelä and E. Ylinen, *Ann. Acta. Sci. Fenn. A* **307**, 2 (1969).
- ¹⁵A. R. Sharp and M. M. Pintar, *J. Chem. Phys.* **53**, 2428 (1970).
- ¹⁶W. Vedder and D. F. Hornig, *J. Chem. Phys.* **35**, 1560 (1961).
- ¹⁷R. C. Plumb and D. F. Hornig, *J. Chem. Phys.* **21**, 366 (1953).
- ¹⁸L. Couture-Mathieu and J. P. Mathieu, *J. Chem. Phys.* **49**, 226 (1952).
- ¹⁹C. C. Stephenson, L. A. Landers, and A. G. Cole, *J. Chem. Phys.* **20**, 1044 (1952).
- ²⁰E. L. Wagner and D. F. Hornig, *J. Chem. Phys.* **18**, 305 (1950).
- ²¹J. R. Durig and D. J. Antion, *J. Chem. Phys.* **51**, 3639 (1969).
- ²²N. E. Schumaker and C. W. Garland, *J. Chem. Phys.* **53**, 392 (1970).
- ²³L. Rimal, T. Cole, and J. Parsons, in *Light Scattering Spectra of Solids*, edited by G. B. Wright (Springer-Verlag, New York, 1968), p. 665.
- ²⁴W. Dultz and H. Ihlefeld, *J. Chem. Phys.* **58**, 3365 (1973).
- ²⁵Michel Couzi, J. B. Sokoloff, and C. H. Perry, *J. Chem. Phys.* **58**, 2965 (1973).
- ²⁶H. G. Smith, J. G. Traylor, and W. Reichardt, *Phys. Rev.* **181**, 1218 (1969).
- ²⁷H. C. Teh and B. N. Brockhouse, *Phys. Rev. B* **3**, 2733 (1971).
- ²⁸H. C. Teh and B. N. Brockhouse, *Phys. Rev. B* **8**, 3928 (1973).
- ²⁹Y. Yamada, Y. Noda, J. D. Axe, and G. Shirane, *Phys. Rev. B* **9**, 4429 (1974).
- ³⁰K. Parlinski, *Acta Phys. Pol.* **35**, 223 (1969).
- ³¹J. Govindarajan and T. M. Haridasan, *Indian J. Pure Appl. Phys.* **8**, 376 (1970).
- ³²H. Jex, *Phys. Lett. A* **34**, 118 (1971).
- ³³H. Jex, *Solid State Commun.* **9**, 2057 (1971).
- ³⁴E. R. Cowley, *Phys. Rev. B* **3**, 2743 (1971).
- ³⁵H. C. Teh, *Can. J. Phys.* **50**, 2807 (1972).
- ³⁶C. H. Kim, Hamid A. Rafizadeh, and Sidney Yip, *J. Chem. Phys.* **57**, 2291 (1972).
- ³⁷J. B. Sokoloff and J. M. Loveluck, *Phys. Rev. B* **7**, 1644 (1973).
- ³⁸J. M. Rowe, J. J. Rush, N. Vagelatos, D. L. Price, D. G. Hinks, and S. Susman, *J. Chem. Phys.* **62**, 4551 (1975).
- ³⁹B. N. Brockhouse, S. Hautecler, and H. Stiller, in *Interaction of Radiation with Solids*, edited by R. Strumane *et al.* (North-Holland, Amsterdam, 1963).
- ⁴⁰A. D. B. Woods, W. Cochran, and B. N. Brockhouse, *Phys. Rev.* **119**, 980 (1960).
- ⁴¹G. Dolling, R. A. Cowley, C. Schittenhelm, and I. M. Thorson, *Phys. Rev.* **147**, 577 (1966).
- ⁴²G. Raunio and S. Rolandson, *J. Phys. C* **2**, 1013 (1969).
- ⁴³B. G. Dick and A. W. Overhauser, *Phys. Rev.* **112**, 90 (1958).
- ⁴⁴G. Dolling and J. L. T. Waugh, in *Lattice Dynamics*, edited by R. F. Wallis (Pergamon, Oxford, 1965), p. 19.
- ⁴⁵U. Schröder, *Solid State Commun.* **4**, 347 (1966).
- ⁴⁶V. Nüsslein and U. Schröder, *Phys. Status Solidi* **21**, 309 (1967).
- ⁴⁷J. S. Reid, T. Smith, and W. L. J. Buyers, *Phys. Rev. B* **1**, 1833 (1970).
- ⁴⁸J. R. Tessman, A. H. Kahn, and W. Shockley, *Phys. Rev.* **92**, 890 (1963).
- ⁴⁹S. Haussühl, *Z. Kristallogr.* **138**, 177 (1973).
- ⁵⁰D. F. Gibbs and M. Jarman, *Philos. Mag.* **7**, 663 (1962).

⁵¹R. A. Cowley, Proc. R. Soc. A 268, 121 (1962).

⁵²J. J. Rush, J. M. Rowe, and N. Vagelatos (unpublished).

⁵³N. Vagelatos, J. J. Rush, and J. M. Rowe (unpub-

lished).

⁵⁴G. Gilat and L. J. Raubenheimer, Phys. Rev. 44, 390 (1966).